



Influence of geological parameters on CO₂ storage prediction in deep saline aquifer at industrial scale

Sarah Bouquet, Dominique Bruel, Chantal de Fouquet

► To cite this version:

Sarah Bouquet, Dominique Bruel, Chantal de Fouquet. Influence of geological parameters on CO₂ storage prediction in deep saline aquifer at industrial scale. TOUGH Symposium 2012, Sep 2012, Berkeley, United States. pp.NA. hal-00777894

HAL Id: hal-00777894

<https://hal-mines-paristech.archives-ouvertes.fr/hal-00777894>

Submitted on 18 Jan 2013

HAL is a multi-disciplinary open access archive for the deposit and dissemination of scientific research documents, whether they are published or not. The documents may come from teaching and research institutions in France or abroad, or from public or private research centers.

L'archive ouverte pluridisciplinaire **HAL**, est destinée au dépôt et à la diffusion de documents scientifiques de niveau recherche, publiés ou non, émanant des établissements d'enseignement et de recherche français ou étrangers, des laboratoires publics ou privés.

INFLUENCE OF GEOLOGICAL PARAMETERS ON CO₂ STORAGE PREDICTION IN DEEP SALINE AQUIFER AT INDUSTRIAL SCALE

Sarah Bouquet, Dominique Bruel, and Chantal de Fouquet

Mines ParisTech, Geosciences Centre
35, rue Saint Honoré
Fontainebleau, 77305 Cedex France
e-mail: sarah.bouquet@mines-paristech.fr

ABSTRACT

Here we examine the consequences of uncertainty with respect to geological parameters, using large-scale 2D models. We also investigate ways to reduce prediction uncertainty, either by showing how a parameter's influence is negligible for a given project design, or by showing for which parameters additional data will significantly increase the quality of prediction. TOUGH2/ECO2N is used to simulate the injection of millions of tonnes of CO₂ for the specific case of the Dogger Aquifer (a carbonate aquifer in the Paris Basin), which has substantial lateral and vertical heterogeneities and few associated data. The parameters of interest are spatial variability and correlation length of permeability, absolute permeability, pore compressibility, cap rock permeability, and relative permeability curves. Several numerical models of permeability are constructed: two uniform cases (two values of permeability) and 200 geostatistical initial realizations, which are modified according to the studied parameters. Results are compared in terms of propagation of pressure perturbations, injectivity (pressure in the vicinity of the well), and gas migration and dissolution. The results indicate that:

(1) The pore compressibility, and the absolute value and spatial variability of permeability have the strongest influence on pressure propagation and injectivity. Relative permeability curves and correlation lengths have a weaker influence at the peak of pressure, but tend to increase the variations in maximum/minimum cases.

(2) Relative permeability curves and heterogeneities have a significant impact on prediction of gas dissolution and migration.

Finally, we also investigate the possibility of reducing the number of simulations.

INTRODUCTION

In terms of available volume, deep saline aquifers seem suitable for CO₂ storage projects at industrial scale, yet the perturbations resulting from the injection of millions of tonnes of CO₂ will constrain the storage capacity of these aquifers. The extent and intensity of these perturbations, as well as CO₂ plume migration, will depend on the geological characteristics of the reservoir. However, the scarcity of data related to these aquifers leads to uncertain predictions of realistic injectivity and storage capacity.

At the regional scale, several storage projects may be involved in the same groundwater system. Therefore the quality of predictions in large-scale studies is critical to insure the feasibility of these projects.

Several studies at basin scale, such as Nicot (2008), Birkholzer et al. (2009), Zhou et al. (2010), Person et al. (2010), have shown that pressure buildup due to massive injection may extend far from the injection point, causing issues in terms of capacity (e.g., pressure interferences between neighboring sites) and posing risks for natural groundwater resources. Some of these studies have also described the influence of pore compressibility, reservoir permeability, and cap rock permeability on pressure-perturbation results at large scale. Depending on the specific study and model used—especially for homogeneous or layered models—boundary conditions (open/closed systems), permeability, and pore compressibility will have a decisive impact on pressure perturbations, especially compared to other parameters such as porosity, temperature, residual gas saturation, anisotropy, or cap rock permeability—as indicated by Buscheck et al. (2012), Schäfer et al. (2011), Chadwick et al. (2010), Flett et al. (2005).

The purpose of this study is to compare the consequences of uncertainty prediction for these influential parameters, as well as to evaluate the consequences of uncertainties in less-studied geological parameters, such as spatial variability of permeability and relative permeability curves. The spatial variability of permeability is much more likely than an assumption of a homogeneous reservoir, but its description is highly uncertain, and injectivity will be strongly affected by such variability as shown by Heath et al. (2012). By determining fluid mobility, relative permeability curves may constrain injectivity and, in turn, predictions of capacity.

METHODOLOGY

Modeling approach

Our models are representations of the Dogger Aquifer (Paris Basin, France), which is a highly heterogeneous carbonate reservoir and therefore relevant for studying the influence of heterogeneity uncertainties. Numerical simulations are performed with TOUGH2/ ECO2N code (Pruess et al., 1999). Outputs from numerical simulations are analyzed via the R software.

Geometrical configuration

The 2D domains of the simulated system, describing a large-scale system of about 140 km in length, represent a vertical section (154 m) of a horizontal well. Thus, the flow is assumed to be linear and perpendicular to the well. The flow depends on the well length and the reservoir properties (Kawecki, 2000). In order to maintain a realistic well setting, the studied injection period is limited to 1 year.

The injection point, corresponding to a limited section of the horizontal well, is located 21 m above the bottom of the reservoir. The injection rate of the section is equal to 0.185 kg/s. Assuming that the well is several kilometres long, it can be estimated that the total injection rate would be equivalent to several million tonnes a year.

The mesh of the models is irregular, with fine discretization around the well ($7 \times 7 \times 7$ m grid-blocks in the vicinity of the injection point, $14 \times 7 \times 7$ m for about 8 km on each side of the well). The length of blocks along the x-direction

increases with increasing distance from the well. The size of blocks in the y- and z-directions remains the same over the entire domain (7×7 m).

Boundary and initial conditions

The simulated domain has closed boundaries. However, the size of the domain is chosen such that the lateral boundaries do not affect the results and therefore are infinite-acting. The domain is considered isothermal (65°C) and initially under hydrostatic conditions (166 bars at the top of the reservoir at 1550 m). The initial salinity is 25 g/L.

Generation of stochastic heterogeneous models

We first generate random, independent, normally distributed variables on a fine, isotropic mesh (cells size: $7 \times 7 \times 7$ m). Then, we apply the moving average method to correlate variables according to a circular variogram with a geometrical anisotropy. For the base case, correlation length in X is 600 m, in Z 20 m. The correlated variables have a Gaussian distribution and are transformed to obtain a log-normal distribution of the permeability values. Finally, for flow simulation, upscaling techniques are applied to the properties in the X direction by using the geometric mean to get the irregular mesh previously described.

Two hundred equi-probable heterogeneous models are built, plus two homogeneous models (two different values of absolute permeability). For all these models, permeability is isotropic ($K_v/K_h=1$). Simulations are conducted using all these representations with the different parameter values.

Geological parameters setting and variations intervals

The spatial variability of permeability is as described above, with a mean at 100 mD, median at 32.4 mD, and standard deviation of $\log_{10}K$ equal to 1.5. The range of 99% of permeability values is $[0.31\text{mD} - 3.16\text{D}]$ which is relevant for Dogger aquifers. Lateral correlation lengths variations are 300 m, 600 m (base case) and 1200 m. Figure 1 illustrates an example of spatial variability representation (heterogeneous models) with different correlation lengths.

In the homogeneous models, the permeability is either equal to the mean of the heterogeneous models (100 mD—mean values are often used to represent the permeability when scarce data are available) or the median value (32.46 mD), which is also the geometric mean, and may represent an equivalent permeability for the entire domain. Porosity is assumed to be uniform in the reservoir and set at 12%.

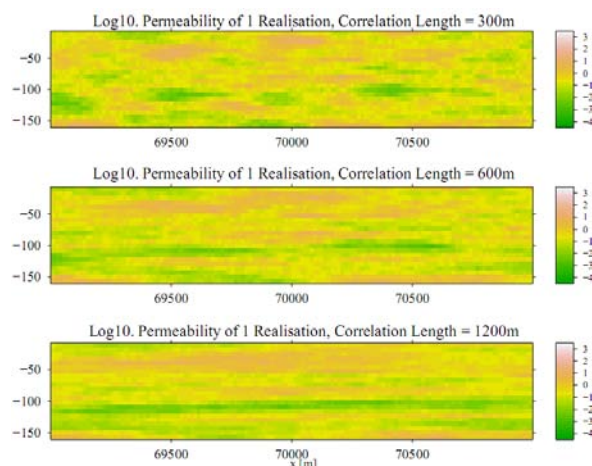


Figure 1. Permeability multipliers (\log_{10} scale) for one model realization with different correlation lengths. Pictures are zoomed in around the well (at $x=70000$ m).

Instead of applying a widely used default value, $4.5E-10Pa^{-1}$, we calculate pore compressibility either by correlation between porosity and pore compressibility for carbonates, or by correlation based on the compressibility measurement function for stress conditions and carbonate rock types ($16.99E-10Pa^{-1}$).

For the relative permeability curves, we use either the Van Genuchten-Mualem and Brooks-Corey methods, or measured data from the Dogger Aquifer (base case, André et al., 2007) or measured data from another carbonate aquifer, the Nisku aquifer (Bennion and Bachu, 2005). For capillary pressure, the same van Genuchten function is used for all scenarios with an entry capillary pressure equal to $5.4E+04$ Pa. In the case of heterogeneous models, Leverett scaling is directly applied via the simulator according to the permeability multiplier.

To study cap rock permeability effects, we focus on three possible cases: (1) impermeable cap

rock (base case, cap rock not represented, and top reservoir boundary closed), (2) a cap-rock permeability of $1E-19m^2$ or (3) a cap-rock permeability $1E-17 m^2$. The thickness of the cap rock is 158 m, and it subdivided into six layers (2×7 m and 4×36 m in height). The cap rock porosity and pore compressibility are 10.5% and $3.48E-10 Pa^{-1}$, respectively. The gas entry pressure is set at $1.5E+07Pa$. Because only a short injection period is considered, diffusion and hysteresis are neglected.

RESULTS AND DISCUSSION

Influence of each parameter in homogeneous and heterogeneous cases on prediction uncertainties

Homogeneous Permeability and Spatial Variability

If permeability increases, the maximum pressure at the well decreases, but the propagation of the pressure-induced disturbance extends further (Figure 2). Nevertheless, heterogeneous cases show higher dispersed results than homogeneous ones. The interval between minimum and maximum behavior of heterogeneous models exhibit homogeneous behavior.

Geological uncertainties in terms of permeability cannot be accounted for through the use of homogeneous models. This realization is even more obvious if we consider the extent of the gas migration in the saturation distributions (Figure 6) obtained from the heterogeneous models. The maximum and mean lateral extents of the CO_2 plume estimated from the 200 heterogeneous realizations are longer than the estimates from both the homogeneous models. This is true even if, for homogeneous models, an increase in permeability implies a longer reach of the plume at the interface between the cap rock and the reservoir.

Correlation length of permeability spatial variability

Pressure perturbations at the well tend to increase with a reduction of the correlation length (Figure 3). On the other hand, variations in the extent of the perturbation increase with the increase in correlation length (the standard

deviation decreases with decreasing correlation length).

However, mean results are close for all correlation lengths, and so the variations in predictions resulting from changes in correlation lengths will mainly affect minimum/maximum cases. Uncertainty with respect to correlation lengths

will affect the reach of the CO₂ plume, with greater lateral extent associated with longer correlation lengths because the preferential pathways would be elongated (Figure 4). As for pressure, the different scenarios yield similar results in terms of the mean extent of CO₂ plume.

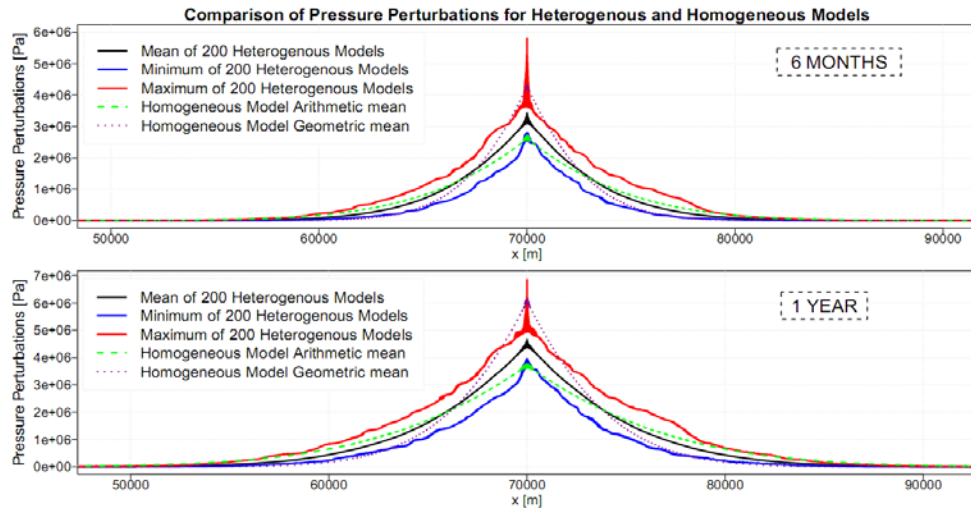


Figure 2. Pressure perturbations results for 200 heterogeneous models (base case, solid lines) and 2 homogeneous models (green and dashed lines: 100mD, purple and dotted lines: 32.4mD).

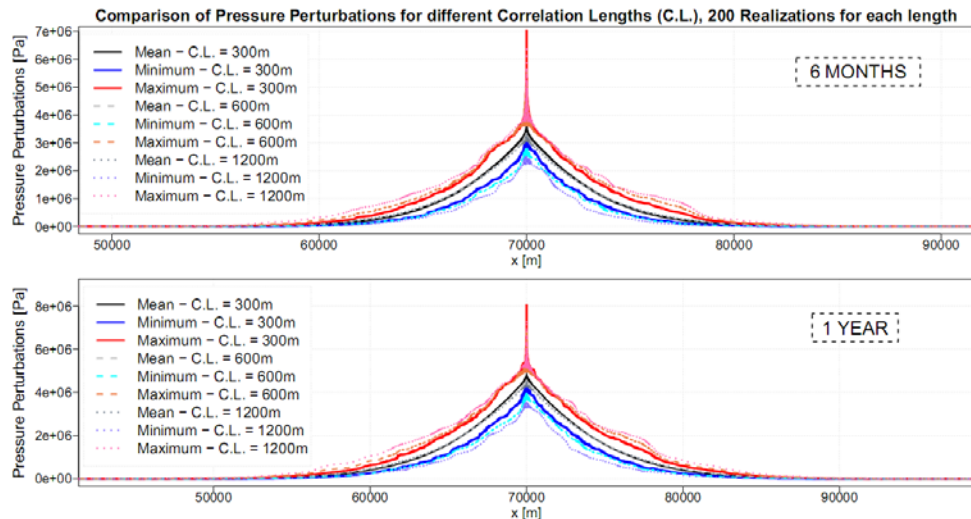


Figure 3. Pressure perturbations results for 200 heterogeneous models with different correlations lengths: 300m, 600m (base case) and 1200m.

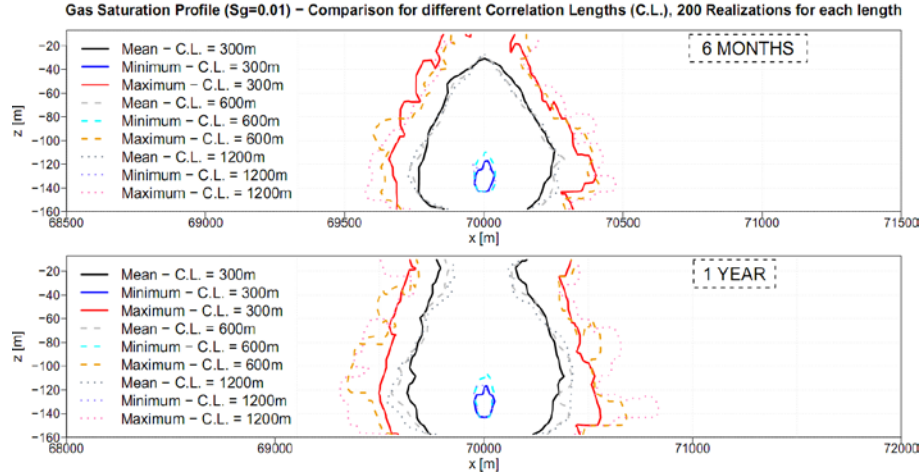


Figure 4. Gas Saturation extension for 200 heterogeneous models with different correlations lengths: 300m, 600m (base case) and 1200m.

Pore Compressibility

Ghaderi et al. (2009) and Schäfer et al. (2011) found that higher pore compressibility increases the injectivity (i.e., decreases the maximum pressure in the well) and slows down the pressure propagation (Figure 5). Therefore, as indicated by the diffusivity equation, pressure propagation would be faster when permeability increases and pore compressibility decreases (Figure 5, right side).

Variations in pore compressibility lead to significant uncertainty in predicting pressure perturbations. For heterogeneous cases (Figure 5, left side), the minimum pressure for the lower pore compressibility is higher than the maximum pressure for the higher pore compressibility. Uncertainty regarding pore compressibility may impact pressure predictions more strongly than heterogeneity uncertainties. Pore compressibility appears to have no influence on gas migration (Figure 6) and dissolution.

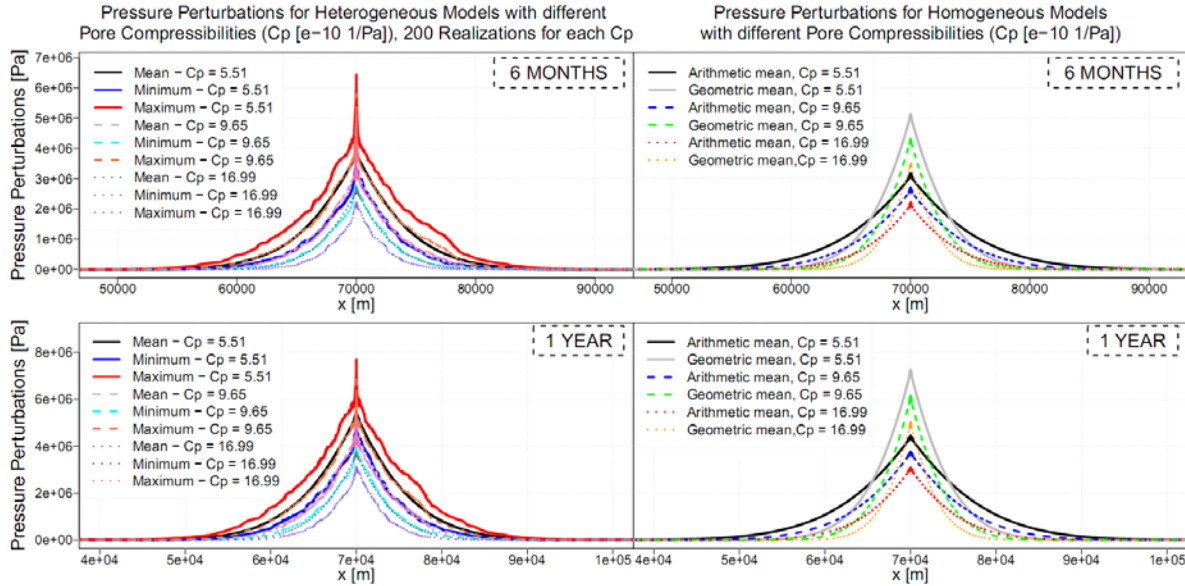


Figure 5. Pressure perturbations for 200 heterogeneous models and 2 homogeneous models with different pore compressibility (solid lines: $5.51 \text{E-}10 \text{Pa}^{-1}$, dashed lines: $9.65 \text{E-}10 \text{Pa}^{-1}$ and dotted lines: $16.99 \text{E-}10 \text{Pa}^{-1}$).

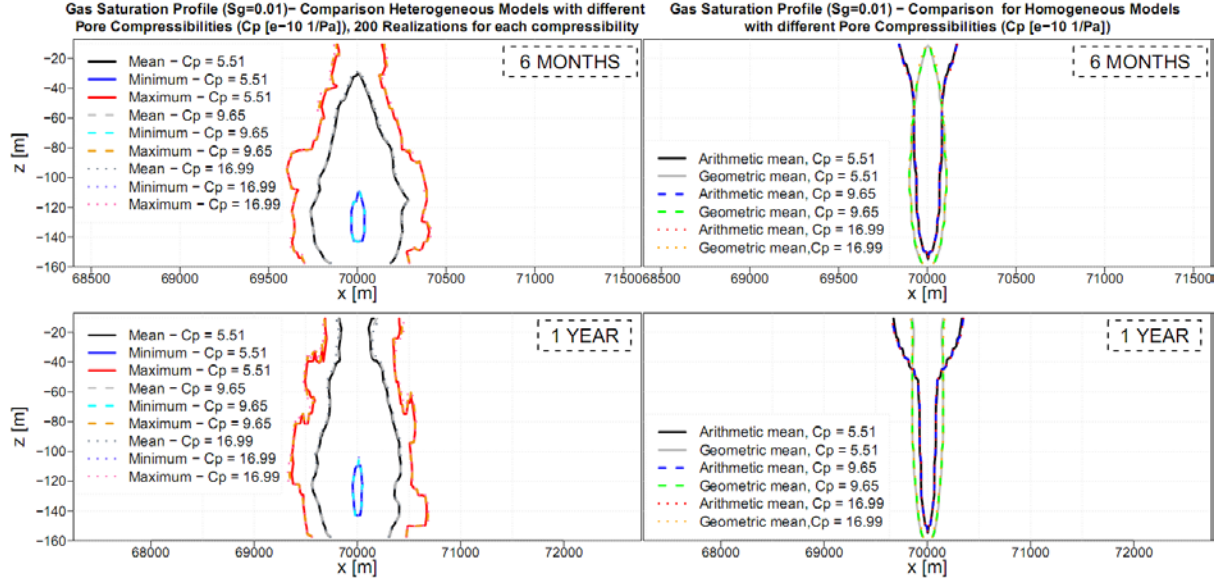


Figure 6. Gas Saturation extension for 200 heterogeneous models and 2 homogeneous models with different pore compressibility (solid lines: $5.51\text{E-}10\text{Pa}^{-1}$, dashed lines: $9.65\text{E-}10\text{Pa}^{-1}$ and dotted lines: $16.99\text{E-}10\text{Pa}^{-1}$).

Cap-rock Permeability

The pressure-perturbation differences between the cases involving impermeable cap rock and low-permeability cap rock ($1\text{E-}19\text{m}^2$) are negligible (Figure 7). However, when the cap-rock permeability is increased to $1\text{E-}17\text{m}^2$, pressure dissipation through the cap rock becomes more significant, and the extent and amplitude of pressure perturbations in the reservoir decrease. Moreover, changes in cap-rock permeability do not affect the reach of the gas saturation front (the simulation results are identical) and supercritical CO_2 does not escape through the cap rock. This is not only because of the low permeability of the cap rock, but also because of its high gas entry pressure. Additionally, the cap rock permeability does not appear to significantly influence the dissolution rate.

With higher cap-rock permeability, more CO_2 could have dissolved at the interface between the top of the reservoir and the cap rock, where supercritical CO_2 , and freshwater in the cap rock coexist. However, the variations in permeability of the impermeable cap rock are lower than 1% and therefore negligible.

Relative permeability curves

Uncertainty over relative permeability curves does not significantly influence pressure- propa-

gation results. However, in maximum cases, because of the decrease in mobility, variations in the relative permeability may exacerbate the maximum peak-pressure behavior in heterogeneous models. The main influence of the relative permeability curves are on the CO_2 plume migration (Figure 8) and dissolution rate.

Comparison of the consequences on predictions from geological uncertainties.

Among all the parameters that have been studied, uncertainty in the pore compressibility has the most significant impact on predictions of pressure perturbation propagation. For a perturbation of 10 bars (Figure 9), estimated propagation differences can reach almost 4 km and have critically important consequences for the injectivity of surrounding wells and for storage capacity predictions. Stochastic dispersion from heterogeneous models can lead to similar uncertainties in the predictions. The differences may even be greater if the correlation length increases. Standard deviation increases with increasing correlation length and with decreasing pore compressibility and cap-rock permeability are associated with the most uncertain predictions.

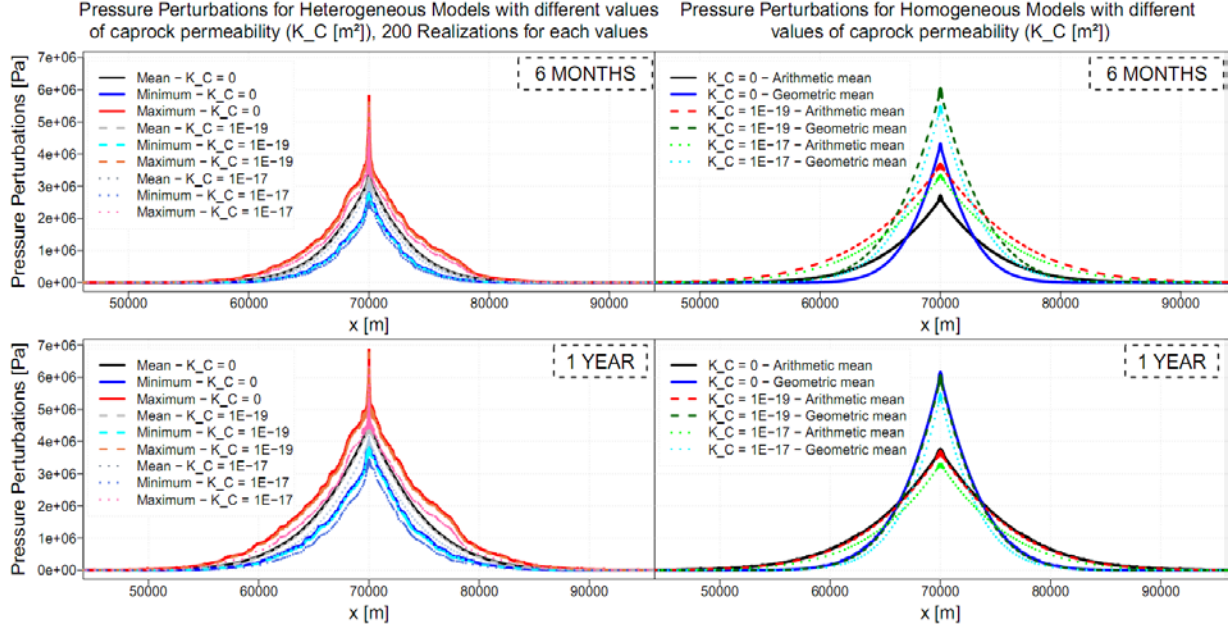


Figure 7. Pressure perturbations results from 200 heterogeneous and 2 homogeneous realizations with different cap-rock permeability (solid lines: Impermeable cap rock, dashed lines: cap-rock permeability = $1\text{E-}19\text{ m}^2$ and dotted lines: cap-rock permeability = $1\text{E-}17\text{ m}^2$).

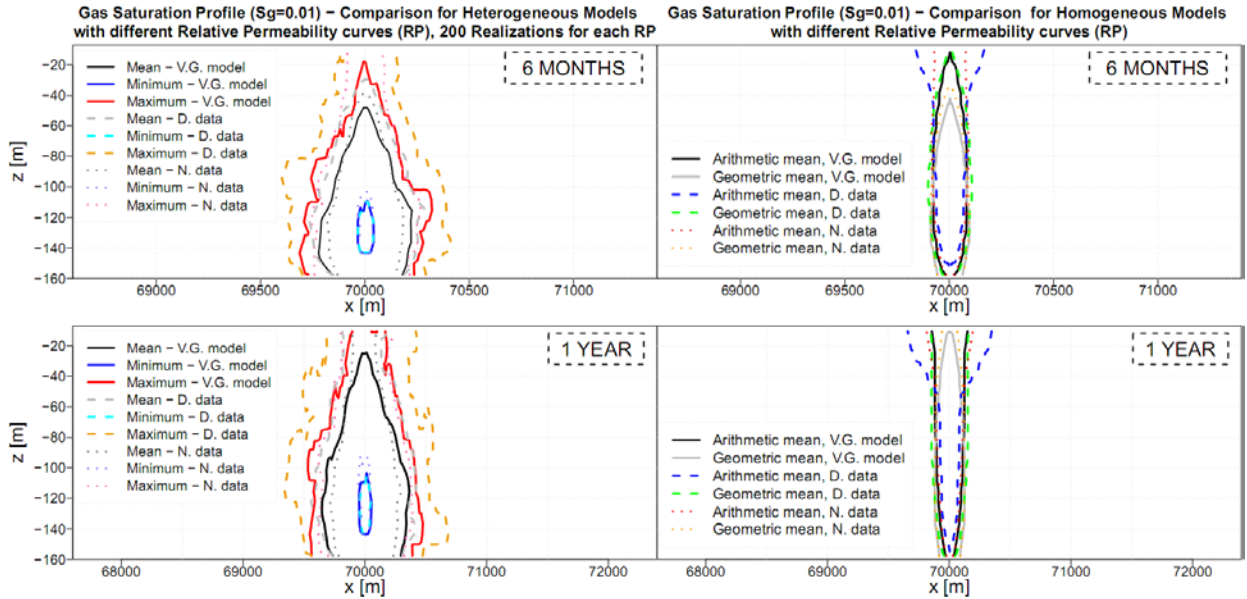


Figure 8. Gas Saturation extension from 200 heterogeneous and 2 homogeneous realizations with different relative permeability curves (solid lines: Van Genuchten-Mualem Model, dashed lines: Dogger aquifer data and dotted lines: Nisku aquifer data).

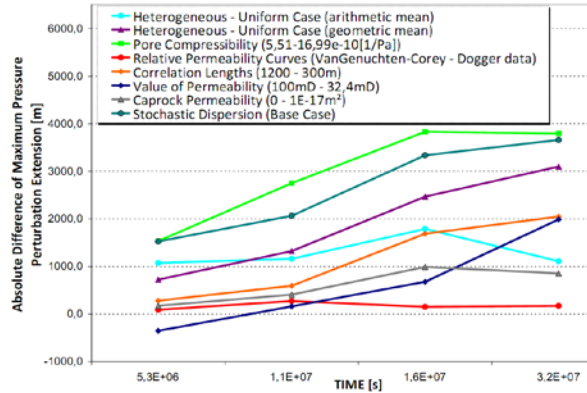


Figure 9. Differences of maximum pressure perturbations (1 MPa) extensions.

Injectivity predictions (i.e., maximum pressure) are less dependent on pore compressibility than on pressure propagation. The absolute values of permeability and heterogeneities uncertainties are the main influences on such predictions. The differences are ~ 28 bars for base-case stochastic dispersion, and ~ 24 bars for homogenous predictions are also influenced by CO_2 mobility: while differences in results between relative-permeability-curve scenarios are usually not as high as those from heterogeneity scenarios, the injectivity can be greatly reduced in some heterogeneous cases because of lower CO_2 mobility.

Dissolution rates (Figure 10) and CO_2 plume migration depend mainly on heterogeneities and the relative-permeability-curve scenarios. The influences of correlation lengths is weaker, and the influence of pore compressibility and cap-rock permeability are negligible.

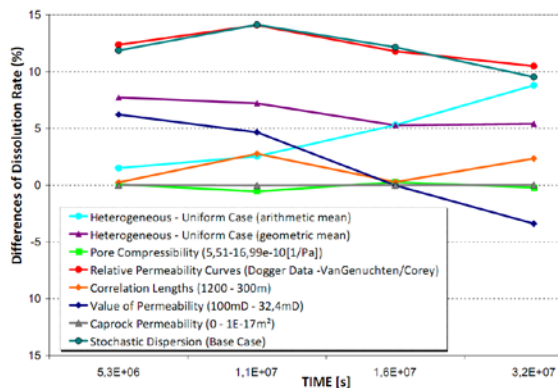


Figure 10. Differences of maximum dissolution rates.

SELECTION OF REALIZATIONS

Based on the pressure results from 200 base-case realizations, we select, at 6 months, the most representative realizations of mean, minimum, and maximum behavior to obtain the same behavior with fewer realizations. This selection (51 realizations) gives equivalent results to those with 200 (Figure 11). Thus, it seems possible to reduce the number of runs for each parameter by a factor of 4. Only 51 realizations need to be run only once, and only up to 6 months, to select a relevant set of realizations for this study.

CONCLUSION

For the large-scale problems and the values of the parameters considered here, uncertainties in pore compressibility and heterogeneities in the permeability appear to have the most effect on the predictions of the extent of the propagation of the pressure and gas saturation disturbances. For risk assessment of leakage (i.e., migration of the plume through fault or abandoned wells) or for the amount of CO_2 trapped, heterogeneities in the permeability of the formation and the cap rock and uncertainties in the relative permeability curves have the most influence on predictions.

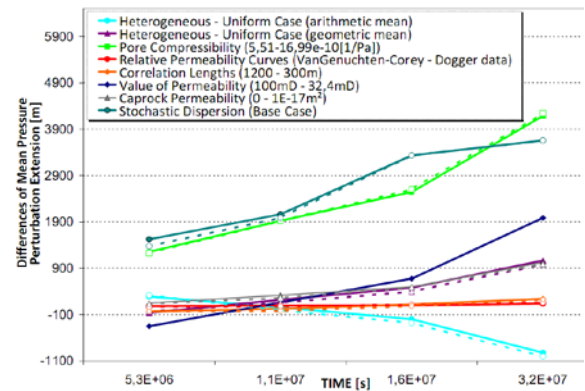


Figure 11. Differences of mean pressure perturbations (1 MPa) extensions (solid lines: 200 realizations, dotted lines with white-filled points: 51 selected realizations).

REFERENCES

- Andre, L., Audigane, P., Azaroual, M. & Menjoz, A., Numerical modeling of fluid-rock chemical interactions at the supercritical CO₂-liquid interface during CO₂ injection into a carbonate reservoir, the Dogger aquifer (Paris Basin, France), *Energy Conversion and Management*, 48, 1782-1797, 2007.
- Bennion, B., Bachu, S., Relative Permeability Characteristics for Supercritical CO₂ Displacing Water in a Variety of Potential Sequestration Zones in the Western Canada Sedimentary Basin, Paper SPE 95547, presented at the 2005 SPE Annual Technical Conference and Exhibition, Dallas, TX, USA, October 9-12, 2005.
- Birkholzer, J.T., Zhou, Q. and Tsang, C.-F., Large-scale impact of CO₂ storage in deep saline aquifers: A sensitivity study on pressure response in stratified systems, *International Journal of Greenhouse Gas Control*, 3, 181-194, 2009.
- Buscheck, T., *et al.*, Active CO₂ reservoir management for carbon storage: Analysis of operational strategies to relieve pressure buildup and improve injectivity, *International Journal of Greenhouse Gas Control*, 6, 230-245, 2012.
- Chadwick, R.A., Noy, D.J. & Holloway, S., Flow processes and pressure evolution in aquifers during the injection of supercritical CO₂ as a greenhouse gas mitigation measure. *Petroleum Geoscience*, 15, 59-73, 2009.
- Flett, M.A., Gurton, R.M. and Taggart, I.J., Heterogeneous saline formations: Long-term benefits for geo-sequestration of greenhouse gases. *Proc 7th Intl Conf on Greenhouse Gas Control Technologies September 2004 Vancouver Canada*, I, 501-509, 2005.
- Heath, J.E., Kobos, P.H., Roach, J.D., Dewers, T.A. & McKenna, S.A., Geologic Heterogeneity and Economic Uncertainty of Subsurface Carbon Dioxide Storage. *SPE Economics & Management*, 4, 32-41, 2012.
- Horne, R.N., *Modern Well Test Analysis: A Computer-Aided Approach*, Petroway Inc, Palo Alto, CA, 1990.
- Jalalh, A.A., Compressibility of porous rocks: Part II. New relationships. *Acta Geophysica*, 54, 399-412, 2006.
- Kawecki, M.W., Transient Flow to a Horizontal Water Well, *Ground water*, 38, 842-850, 2000.
- Nicot, J.-P., Evaluation of large-scale CO₂ storage on fresh-water sections of aquifers: An example from the Texas Gulf Coast Basin, *International Journal of Greenhouse Gas Control*, 2, 582-593, 2008.
- Person, M. *et al.*, Assessment of basin-scale hydrologic impacts of CO₂ sequestration, Illinois basin, *International Journal of Greenhouse Gas Control*, 4, 840-854, 2010.
- Pruess, K., C. Oldenburg, and G. Moridis, *TOUGH2 User's Guide, Version 2.0*, Report LBNL-43134, Lawrence Berkeley National Laboratory, Berkeley, Calif., 1999.
- Schäfer, F., Walter, L., Class, H. & Müller, C., The regional pressure impact of CO₂ storage: a showcase study from the North German Basin, *Environmental Earth Sciences*, 65, 2037-2049 2011.
- Zhou, Q., Birkholzer, J.T., Mehnert, E., Lin, Y.-F. & Zhang, K, Modeling basin- and plume-scale processes of CO₂ storage for full-scale deployment, *Ground water*, 48, 494-514, 2010.